# Membrane Diffusion III: Influence of Solvent Composition and Permeant Solubility on Membrane Transport

G. L. FLYNN▲ and R. W. SMITH

**Abstract** □ Phenomena associated with membrane permeability are important pharmaceutically in drug-transport modeling and in the design of effective drug delivery systems. In the present study, it was found that under certain predetermined conditions the steady-state transfusion of dimethylpolysiloxane membranes by *p*-aminoacetophenone from binary solvent mixtures was essentially controlled by the thermodynamic activity of the compound in the applied phase. This study augments and supplements present theories concerning drug transport, and it sharply contrasts with previous work where "drug delivery" was maximized at the coincidence of complete solubility and saturation for a fixed ratio of drug and mixed solvent and varying ratio of solvents. Under the conditions of these experiments, specific effects of solvent on mass transport were limited to slight changes in apparent diffusivity, $D'$. The $D'$ values were calculated from lag times obtained by the Daynes and Barrer extrapolation. Application of these concepts to some practical drug-transport situations is discussed.

**Keyphrases** □ Drug transport—effect of solvent and solubility, *p*-aminoacetophenone across dimethylpolysiloxane membranes □ Membrane diffusion—thermodynamic activity of the diffusing compound in the applied phase □ Topical drug availability—thermodynamic control □ Dimethylpolysiloxane membranes—diffusion of *p*-aminoacetophenone □ *p*-Aminoacetophenone—diffusion across dimethylpolysiloxane membranes

The multifarious applications of membrane technology include practical usage in separations to highly technical and theoretical considerations such as are found in drug-transport modeling. In general, two distinctly different phenomenological mechanisms are involved in the flow of materials through thin barriers; these are dialysis or passage of mass through macroscopic pores filled with solvent and molecular transport involving dissolution of the permeant into the barrier followed by molecular diffusion across it. Under select conditions, membranes operating principally by either of these mechanisms can be semipermeable and find usage in separation chemistry. The distinction that selective diffusion in dialysis depends mostly on molecular size while in molecular transport relative solubilities in the barrier and absolute solubilities in the donor phase are controlling is an important one. As pointed out previously (1), the dimethylpolysiloxane membranes used in these experiments belong in the latter category.

Because of the ubiquitousness and strategic biological importance of membranes, many and diverse experimental systems have been devised to shed light upon their properties. *In vitro* literature studies are of several types, including studies using a fluid lipid phase and experiments with continuous polymeric films. Doluisio and Swintosky (2) introduced the former as a three-phase system having a fluid lipid phase making two interfaces with aqueous compartments. Later modifications of this basic design were published by several authors (3, 4). In all cases, all the phases are stirred, leading to several readily apparent experimental deficiencies. There is no concentration gradient in the "membrane" itself and, as pointed out by Perrin (5), the relative volumes of the phases influence the rate of appearance in the receptor compartment. In actuality, these studies amount to the determination of rates of partitioning, and a two-phase system can serve equally well in determining transference rates (6). Since the barrier in such systems is a liquid–liquid interface, the dimensions of cellular membranes are reasonably approximated. However, there is no structural integrity to the interface; that is, molecules are free to diffuse into and out of the barrier, and this leads to a major dissimilarity with respect to the cellular situation.

The second classification mentioned amounts to the use of relatively thick (>25 -μm.), continuous polymeric slabs sandwiched between two fluid and, usually, aqueous compartments. Disappearance of diffusing species from the donor phase or appearance in the receptor phase is followed with respect to time. Mechanical problems involved in optimizing the data obtained from such three-phase (including the membrane) two-compartment systems were discussed (7). From the standpoint of biophase simulation, data from these systems can be misleading due to the extreme thicknesses of the barriers which, under normal conditions, preclude any significant influence on mass transport from penetration into or exit from the barrier (partitioning). In living systems, it is possible that these steps can be contributive because cellular membranes are measurable in molecular dimensions. On the other hand, thick membranes have structural integrity and provide a barrier with an internal gradient. Stirring effects are usually negligible, although not when diffusional layers at the membrane surface contribute to the total barrier (8). When compared to "fluid membrane" systems, relative membrane to compartmental volumes are more closely aligned with the biological case. If macroscopic biological membranes such as the skin or cornea are to be considered, multimicron continuous films offer an opportunity for meaningful *in vitro* approximations.

Dimethylpolysiloxane[1] membranes are particularly suited to drug-transport simulation because of their ease of preparation (9), their hydrophobic character, and the high diffusivities (diffusion constants) obtained in them (1, 9–11). Garrett and Chemburkar (12, 13) published a series of papers showing the facility with which *p*-aminopropiophenone, related phenones, barbiturates, and several other classes of compounds pass through dimethylpolysiloxane barriers. Similarly, Most (9) provided data on the passage of ethyl *p*-aminobenzoate (benzocaine) through dimethylpolysiloxane

[1] Silastic sheeting, Dow Corning, Midland, Mich., Dow Corning Medical Product Bulletin 14-184.

films and, in particular, showed a marked effect on the nonsteady-state transport traceable to the presence of silica filler. Flynn and Roseman (1) expanded on these concepts and provided mathematical relationships governing the influence of the adsorption process. Haleblian *et al.* (11) showed the permeability of dimethylpolysiloxane membranes to chlormadinone acetate, a progestational steroid. Related steroid studies using dimethylpolysiloxane implants and rings were contributed by Sundaram and Kincl (14) and, more recently, Roseman and Higuchi (10). In the cases where the investigators were able to estimate diffusivities, they found them to be large and in the range of $2 \times 10^{-6}$ to $1 \times 10^{-7}$ cm.$^2$/sec.

The present studies are similar to those of Garrett and Chemburkar (12), particularly the studies in which ethanol–water mixtures were used, but have several important differences. A system with a high diffusional area to receptor compartmental volume was used in conjunction with an external spectrophotometric flow cell, the combination of which provided complete tracings of concentration changes and sufficiently greater sensitivity to estimate lag times accurately. Apparent diffusivities were calculated along with steady-state permeabilities and fluxes. Furthermore, diffusional studies were performed with an incremental increase in the donor propylene glycol–water ratio, and the influence of vehicle solubility and solvent was determined. The physical significance of the various diffusional factors are examined and discussed with respect to drug transport, with particular reference to the behavior of topically applied medicaments.

## EXPERIMENTAL

**Materials**—*p*-Aminoacetophenone[2] was used as received or, alternatively, crude *p*-aminoacetophenone was repetitively crystallized, until colorless, from warm *n*-propanol filtrates after treatment with activated charcoal. Deionized water and propylene glycol USP were used to prepare the solvent systems. Dimethylpolysiloxane membranes of varied thicknesses were conditioned as described by Flynn and Smith (7). Their actual thicknesses were determined by the method of Garrett and Chemburkar (12).

**Diffusion Cell Operation and Data Acquisition**—The particulars of operation of the diffusion cell assembly such as pumping flow rate, compartmental volumes, and membrane area were presented previously (7). Stirring was maintained at 60 r.p.m. for all experiments. Estimation of lag times was accomplished by extrapolation of the steady-state portion of the curves to zero absorbance, the initial absorbance, and measuring to the nearest $^1/_{64}$ of an inch the distance from the start of the run to the steady-state intercept. Chart speeds were 1 min./in. for the 126-$\mu$m. membrane and 10 min./in. for the thicker membranes, allowing measurement of lag times to the nearest 1 or 10 sec., respectively. An averaged mechanical lag time, the time for the contents of the cell to be pumped into the light-path of the spectrophotometer, of 1.25 min. was determined, and this value was subtracted from each gross lag time value to obtain the true lag time. Care obviously had to be taken to mark the moment of initiation of each run. The progress of all runs was monitored continuously by the use of an external flow cell mounted in a Beckman DB spectrophotometer. All runs were repeated, and the data given are averaged values.

**Preparation of Samples**—For the studies on steady-state permeability as a function of concentration, an excess of *p*-aminoacetophenone was added to a large flask of deionized water. After stirring for roughly a day at room temperature, the excess compound was filtered off and the indicated dilutions were made. Their concentrations were expressed in terms of percent of room temperature saturation. These solutions were placed in the donor compartment of the diffusion cell maintained at 37°, and the permeabilities were estimated. The runs were followed at 310 nm. and, to assure sink conditions, 0.1 *N* HCl was used as the receptor phase

Prior to preparing the mixed solvent solutions for subsequent runs, an excess of *p*-aminoacetophenone was placed in 50 ml. of an equal volume mixture of propylene glycol and water and stirred for approximately 50 hr. at 37° to obtain an equilibrium concentration. A 1.0-ml. sample was removed with a glass wool-tipped pipet and assayed spectrophotometrically after appropriate dilution. Approximately 4.25 g. of compound dissolved in the 50 ml. of solvent mixture. This amount of compound (4.25 g.) was placed in each of a series of 50-ml. glass-stoppered conical flasks. Successive 5-ml. incremental increases in propylene glycol were added to each flask by syringe. Fifty milliliters was placed in the last flask. Similarly, but skipping the last flask and in the reverse direction, 5-ml. incremental increases in water were added to the respective flasks, bringing the total solvent volume added to each to 50 ml. These were placed in a 37° water bath equipped with a shaking apparatus and allowed to equilibrate for several days. The 37° solutions or suspensions were quickly transferred to the donor compartment of the diffusion cell, and the runs were commenced. A similar method of sample preparation was used for runs aimed at assessing the effect of membrane thickness on the rate of transport. Deionized water constituted the receptor phase. Therefore, in the context of this report, the word "donor" signifies the applied phase or phase of high concentration, while the term "receptor" identifies the phase into which the diffusing species is collected and analyzed.

**Determination of Solubilities**—One-milliliter samples were removed from the incubated propylene glycol–water mixtures with a glass wool-tipped pipet and assayed spectrophotometrically, after appropriate dilution, on a Cary 11 recording spectrophotometer. Calculated solubilities were based on the previously determined molar absorptivity of 16,800 ± 100 at 310 nm. Above 50% propylene glycol, all the permeant was solubilized and, therefore, the theoretical concentration of 85 mg./ml. was assumed.

**Calculations**—Steady-state slopes were obtained graphically in units of absorbance per minute. These were converted to total steady-state flux, $Q_T$, in milligrams per second by Eq. 1, using an independently determined molar absorptivity, $a_m$, of 16,800, a receptor cell volume of 17.8 ml., and the molecular weight, $MW$:

$$Q_T = \frac{(A/\text{min.}) \times 0.178 \times MW}{a_m \times 60} = \text{mg./sec.} \qquad \text{(Eq. 1)}$$

The apparent permeability coefficient, $P'$, was calculated from:

$$P' = Q_T \times \frac{h}{AC^0} \qquad \text{(Eq. 2)}$$

where $h$ is the membrane thickness, $A$ is the cross-sectional areas (10 cm.$^2$), and $C^0$ represents the concentration in milligrams per milliliter in the applied phase. Apparent diffusivities were obtained from the lag time relationship of Daynes (15) and Barrer (16):

$$D' = \frac{h^2}{6t_L} \qquad \text{(Eq. 3)}$$

where $D'$ represents the apparent diffusivity, and $t_L$ is the corrected extrapolated lag time. Apparent partition coefficients, represented by $k_{app.}$, were obtained from the ratio of $P'$ to $D'$. Steady-state fluxes per unit area, $Q$, are used in the tables and graphs, and these are exactly an order of magnitude less than the total steady-state flux due to the 10-cm.$^2$ membrane cross-sectional area. The experiment analyzing flux as a function of concentration was used as a check on the operation of the system, and these data were not reduced to the more fundamental units.

## THEORETICAL

The present diffusional system is a simple three-phase design: donor compartment, membrane, and receptor compartment. A schematic representation is presented in Fig. 1 using actual relative dimensions of the cell compartments and membrane. In such systems, the resistance of the total barrier is a sum of the resistances of individual barriers in the laminate, much as resistances are additive for

[2] Eastman Organic Chemicals.

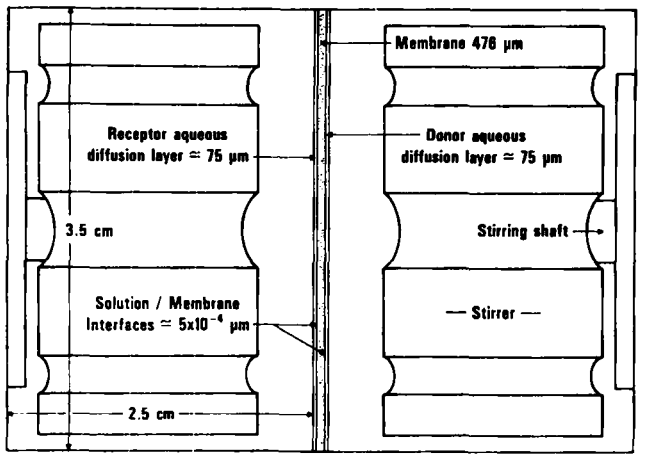


**Figure 1**—*Relative diffusion cell and barrier dimensions.*

electrical resistors in series. Individual resistances are inversely proportional to individual barrier permeabilities. The potential barriers to flow (namely, the membrane, the diffusional layers contiguous to each side of the membrane, and the membrane–solution interfaces) are identified dimensionally in Fig. 1. To interpret results, it is necessary to determine where the actual resistance arises in the total barrier. The total resistance for steady-state permeation of a membrane in the three-phase system is described by Eq. 4 (17):

$$R = \frac{2h_w}{D_w} + \frac{2h_i}{D_i} + \frac{h_m\tau}{D_m k_p V_1} \qquad \text{(Eq. 4)}$$

where $D_w$, $D_i$, and $D_m$ are the specific diffusivities in the solvent (usually water), in the solvent–membrane interface, and in the membrane, respectively; $h_w$, $h_i$, and $h_m$ are the thicknesses of the diffusional layer, solvent–membrane interface, and membrane, respectively; and $k_p$ is the true membrane/applied solvent partition coefficient. For the present cell system, the diffusion layers are presumed to be of equivalent thickness as are the solvent–membrane interfaces as stirring is equidistant from both sides of the membrane, synchronized, and symmetrical. Thus, since there are two membrane interfaces with fluid compartments, the values of two in Eq. 4 are generated. The heterogeneous nature of the dimethylpolysiloxane membranes employed was pointed out previously (1, 9). Since the presence of the silica filler increases the effective diffusional pathlength by a tortuosity factor, $\tau$, and decreases the volume fraction available for diffusion, $V_1$, these factors have been included in Eq. 4.

The total diffusional system is similar to that described by Stehle and Higuchi (18) in a recent article. These authors neglected the term corresponding to partitioning resistance. When macroscopically thick membranes only are considered, it is extremely unlikely that the interfacial resistance, $2h_i/D_i$, would contribute significantly to the total resistance, even if $D_i$ were relatively small, because $h_i$ is of molecular dimensions and is orders of magnitude[3] less than $h_w$ or $h_m$. This is true for the present dimethylpolysiloxane membranes, which ranged from about 75 to about 1000 μm., but it is not the case when cellular membranes, which are roughly 60 Å or approximately 10 molecular dimensions thick, are considered. Obtaining the energy and orientation to pass through the unsymmetrical force field at the interfaces may contribute to the total barrier property in a cellular system.

Contributions to barrier function from the diffusion layers are not so easily dismissed. The specific diffusion constant at 37° for the "prototype diffusant," *p*-aminoacetophenone, is $2.44 \times 10^{-6}$ cm.²/sec. (1) and is within a factor of 3 of the diffusion constant in water calculated from the Einstein equation, $6.57 \times 10^{-6}$ cm.²/sec. If the partition coefficient were close to 3, $1/D_w$ would be approximately equal to $1/D_m k_p$ and the contribution to the barrier would be directly dependent on the relative thicknesses of its parts. However, the true partition coefficient was previously determined to be $3.21 \times 10^{-2}$ (1), causing $1/D_m k_p$ to be two orders of magnitude less than $1/D_w$. Since the membranes used were about 500 μ thick and diffusion layers are generally an order of magnitude less than this (8) (0–100 μm.), the contribution of diffusion layers would not be appreciable in these studies.

[3] As used here, an order of magnitude is a factor of 10.

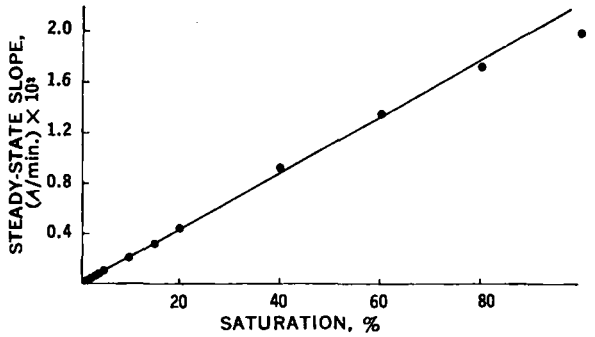


**Figure 2**—*Plot showing the linear relationship between the steady-state slope and donor phase concentration (expressed in terms of percent saturation at 25°) at 37°.*

Since the total barrier function is attributable to the membrane, the steady-state flux, $Q$, for a given run is described by (1):

$$Q = D_m k_p \frac{V_1}{\tau h_m} C^0 \qquad \text{(Eq. 5)}$$

when the receptor compartment is a sink and $D_m$ is independent of concentration. The $V_1$ in this expression is the continuous phase volume fraction. Higuchi (19) put this equation into thermodynamic terms by substituting the activity for concentration and the activity coefficient ratio for the partition coefficient (19):

$$Q = D \frac{V_1}{\tau h_m} \frac{a_D}{\gamma_m} \qquad \text{(Eq. 6)}$$

where $a_D$ is the activity in the applied phase, and $\gamma_m$ is the activity coefficient in the membrane. This equation states that mass transport across a membrane is directly dependent on the activity of the permeant in the "vehicle" or applied phase. The present study was designed to substantiate experimentally this fundamental concept. In the remainder of the paper, the subscript $m$ will be dropped because all further discussion will be concerned with the membrane properties only.

The apparent diffusivities, $D'$, and apparent partition coefficients, $k_{app.}$, were determined for each run. Both were defined previously in terms of more fundamental diffusional parameters (1). The $D'$ values serve as a check on membrane integrity. Variances would be attributable to changes in adsorption and/or changes in the polymer itself. These can be distinguished by examining the behavior pattern of

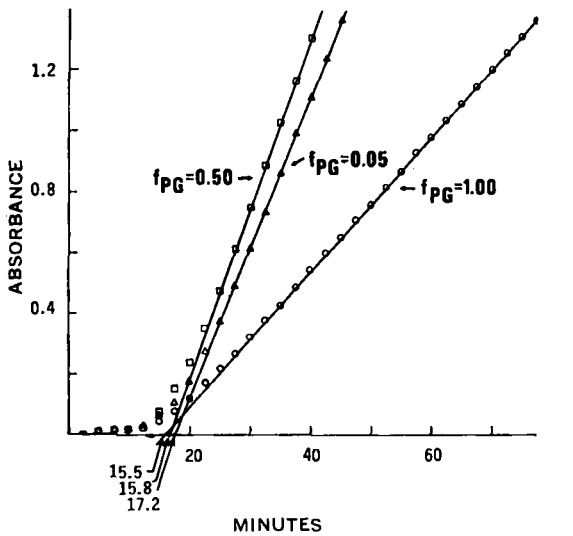


**Figure 3**—*Plot showing absorbance changes as a function (time) for three propylene glycol fractions. Key: △, 0.05; □, 0.50; and ○, 1.00. Data were taken from continuous tracings of the diffusional runs.*

**Table I**—Compilation of Measured and Calculated Diffusional Parameters for Runs Assessing the Effect of Increasing the Propylene Glycol Volume Fraction

| Propylene Glycol Volume Fraction, $f_{PG}$ | Membrane Thickness[a], in. × $10^3$ | Averaged[b] Applied Phase Concentration, mg./ml. | Averaged[b] Steady-State Flux, mg./cm.²/sec. × $10^5$ | Averaged[b] Corrected[c] Lag Time, min. | Averaged[b] $P$, cm.²/sec. × $10^9$ | Averaged[b] Apparent Diffusivity, $D'$, cm.²/sec. × $10^7$ |
|---|---|---|---|---|---|---|
| 0.05 | — | 12.71 | 1.39 | 16.42 | 51.9 | 3.84 |
| 0.10 | — | 15.62 | 1.43 | 15.94 | 43.6 | 3.95 |
| 0.15 | — | 18.89 | 1.42 | 16.49 | 34.9 | 3.82 |
| 0.20 | — | 23.47 | 1.37 | 15.77 | 27.8 | 4.00 |
| 0.25 | — | 28.80 | 1.48 | 14.94 | 24.4 | 4.22 |
| 0.30 | 19.00 | 35.58 | 1.47 | 16.19 | 19.6 | 3.89 |
| 0.35 | 18.84 | 44.14 | 1.53 | 15.46 | 16.5 | 4.08 |
| 0.40 | 18.40 | 56.08 | 1.47 | 15.93 | 12.5 | 3.95 |
| 0.45 | 18.40 | 71.16 | 1.48 | 15.21 | 9.91 | 4.14 |
| 0.50 | 18.94 | 85.64 | 1.41 | 14.76 | 7.85 | 4.27 |
| 0.55 | 18.50 | 85.0[d] | 1.37 | 14.45 | 7.66 | 4.36 |
| 0.60 | 18.94 | 85.0[d] | 1.21 | 14.45 | 6.76 | 4.36 |
| 0.65 | 18.65 | 85.0[d] | 1.07 | 15.15 | 6.01 | 4.16 |
| 0.70 | 18.96 | 85.0[d] | 1.07 | 14.78 | 6.01 | 4.26 |
| 0.75 | 18.48 | 85.0[d] | 0.93 | 15.15 | 5.19 | 4.16 |
| 0.80 | 18.58 | 85.0[d] | 0.90 | 15.60 | 5.05 | 4.04 |
| 0.85 | 18.86 | 85.0[d] | 0.80 | 14.90 | 4.47 | 4.23 |
| 0.90 | 18.88 | 85.0[d] | 0.77 | 14.45 | 4.28 | 4.36 |
| 0.95 | 19.02 | 85.0[d] | 0.71 | 13.43 | 3.95 | 4.69 |
| 1.00 | 18.87 | 85.0[d] | 0.60 | 13.98 | 3.37 | 4.51 |

[a] For the latter half of the second of set runs, average of six individual readings. [b] Average of two independent measurements. [c] Corrected by subtracting mechanical lag time of 1.25 min. [d] Theoretical amount—total solution.

steady-state flux, which would change only if the effect were on polymer permeability. Since the apparent partition coefficient is directly proportional to the true partition coefficient, changes in the true partition coefficient as a function of solvent ratio would be accurately reflected in its hybrid counterpart, assuming, of course, a constant filler volume fraction, $V_2$, and a fixed adsorption interaction constant, $K$. These conditions were reasonably met in the current studies.

## RESULTS

In Fig. 2, steady-state fluxes at 37° in absorbance units per minute for a series of dilutions prepared from a room temperature saturated solution are plotted against the percent of saturation at the lower temperature. A necessary consequence of Fickian diffusion is that a linear dependency be obtained with concentration under steady-state conditions. These data clearly indicate the dependency to be linear at low concentrations. At higher concentrations, there is some deviation from the expected dependency. This deviation is likely attributable to the appearance of significant solute–solute interactions as the concentration is increased, for these become more and more, resulting in diminished activity coefficients. These data were obtained with 126-μm. membranes and, to assure sink conditions over the full range of concentration, the receptor phase was 0.1 $N$ hydrochloric acid instead of deionized water, which was used in all subsequent runs. Absorbance changes were followed at 310 nm. as in other cases, and this resulted in some loss in sensitivity due to spectral changes accompanying protonation of the *p*-amino moiety. Thus, concentration dependence by this method closely paralleled that previously observed (1).

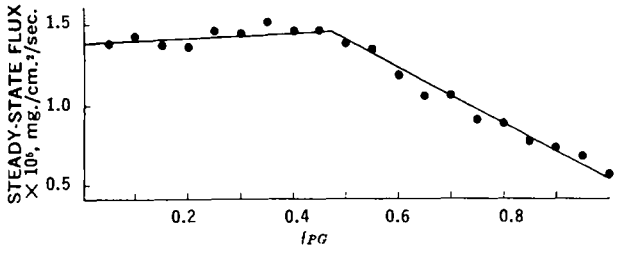


**Figure 4**—*Plot showing the steady-state flux as a function of the propylene glycol fraction,* $f_{PG}$. *The particular shape here is dependent on sample preparation because the coincidence of total solubility and saturation was predetermined to be at* $f_{PG}$ *0.50.*

In Fig. 3, some typical total diffusional curves are presented. These data were obtained from mixed solvent solutions with propylene glycol volume fractions, $f_{PG}$, of 0.05, 0.50, and 1.00, respectively. The curves correspond to absorbance changes at 310 nm. in a 1.0-cm. pathlength flow cell connected to the receptor compartment of the diffusional cell. The obvious change in steady-state permeability in the run using pure propylene glycol indicates a marked influence of solvent on the mass transport process. The virtually common lag times, however, suggest that this influence is not related to large changes in diffusivity within the membrane.

Data obtained from curves similar to those found in Fig. 3 are compiled in Table I for every propylene glycol volume fraction tested. It can be seen that values of the permeability coefficient, $P'$, varied over an order of magnitude at the extreme ends of the range but the actual flux was only roughly halved. This is actually an artifact introduced by the experimental design, a design that predetermined the coincidence of total solubility and saturation to be at a $f_{PG}$ of 0.50, and is not to be considered a general case. In this particular incidence, the decrease in $P'$ as $f_{PG}$ is increased up to 0.50 is offset by a matching increase in donor phase solubility. Past this point, the solution is no longer saturated, the escaping tendency or activity becomes proportional to the fractional saturation, and the steady-state flux falls. These features are readily seen in Fig. 4. Here, the steady-state flux is plotted against the propylene glycol volume fraction. There is a slight increase in slope up to volume fraction 0.50 and a sharp linear decline thereafter.

It can be seen from Table I that there is a slight but erratic increase in lag time as $f_{PG}$ is increased. Values of the apparent diffusivity, $D'$, calculated from the lag time data show a comparable trend. The latter are plotted against $f_{PG}$ in Fig. 5. The statistical line drawn through these points has a correlation coefficient of 0.78 and a sta-

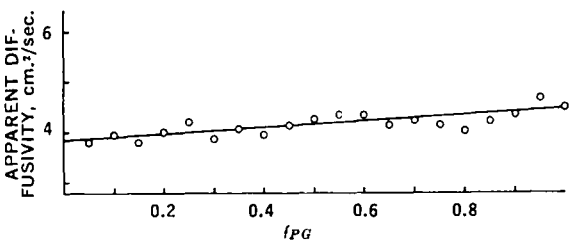


**Figure 5**—*Plot showing a gradual definite increase in apparent diffusivity with increasing propylene glycol fraction.*

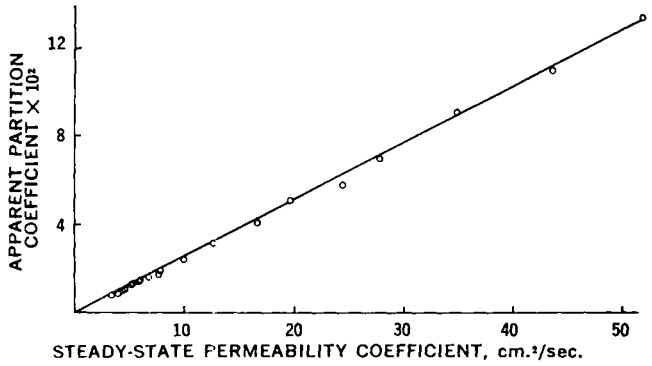


**Figure 6**—*Relationship of apparent partition coefficient,* $k_{app.}$, *to steady-state permeability coefficient,* P, *in a system with essentially invariant* D.

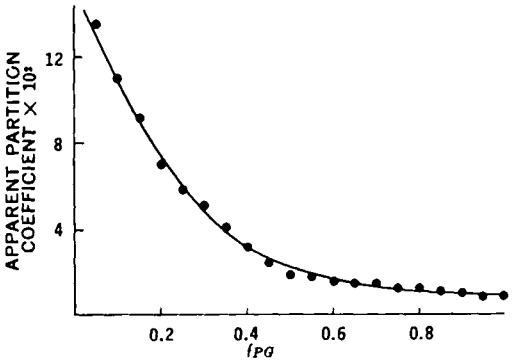


**Figure 7**—*Dependency of apparent partition coefficient,* $k_{app.}$, *on propylene glycol fraction.*

tistically significant slope of $6.00 \times 10^{-8}$ cm.²/sec./unit $f_{PG}$, with a standard deviation in the same units of $1.10 \times 10^{-8}$. It appears as if propylene glycol has a slight but definite effect on membrane integrity, an effect perhaps attributable to its acting as a plasticizer since steady-state permeability is also increased. When the slightly increasing flux up to $f_{PG}$ of 0.5 (Fig. 4) is corrected for changes in $D'$ itself, there is no significant slope to the line drawn through this region. Thus, in this system, as long as a solid–solution drug equilibrium exists in the donor phase, the flux is invariant.

The validity of the present data is predicted on sink conditions existing in the receptor (deionized water) phase. It can be seen from Table I that the donor solution concentration was never less than about 12 mg./ml. Runs were followed to a limiting absorbance of 1.0 or, occasionally with scale expansion, 1.5. Since an absorbance of 1.0 is produced by a solution of only roughly $9 \times 10^{-3}$ mg./ml. concentration (310 nm.), negligible backflow is to be expected and sink conditions were closely approached. Scattering in the accumulated data was evident after the study was well along and since it seemed possible that variation in individual membrane thicknesses could contribute to, or be responsible for, this problem, the thicknesses of each membrane used in the latter portion of the repeat runs were measured. Thickness variations were slight (Table I), and the average thickness, 476 μm. (0.01875 in.) was not appreciably different from that previously reported (7). This new averaged thickness was used in the calculation of apparent diffusivity, $D'$, from the lag times.

In Fig. 6, a plot of calculated apparent partition coefficient values $k_{app.}$, against the experimental values of the apparent permeability constant, $P'$, is presented. This plot has an internal redundancy because $P'$ was used in calculating $k_{app.}$. Nevertheless, the plot has several significant features. It demonstrates the linear dependence of $P'$ on the partition coefficient in a system with relatively invariant $D'$. The reciprocal of the slope of the line drawn through the points generates an averaged $D'$, $4.1 \times 10^{-7}$ cm.²/sec. The high data point density at the lower portion of the plot is attributable to $k_{app.}$ becoming relatively invariant at high propylene glycol fractions (Fig. 7). Since propylene glycol is by far the better solvent for *p*-aminoacetophenone, this outcome is expected.

## DISCUSSION

Any experimental system shedding light on mechanisms and/or relative rates of movement of chemicals into, across, and out of essentially nonpolar barriers is of interest pharmaceutically because of the broad applications of such phenomena in both dosage form design (*e.g.*, implants and vaginal rings) and drug-transport simulation. The significance of the latter aspect is perhaps summed up best by Hogben *et al.* (20), who stated: "there is a sufficient parallel between the rate of adsorption of a drug and the lipid solubility of its unionized form to be consistent with the hypothesis that the intestinal–blood barrier is essentially lipoid in nature." There is evidence that other natural barriers, such as the buccal mucosa (21) and skin (22), act similarly. Comparison of the biological barriers with the dimethylpolysiloxane barriers employed here shows the latter to be of less complexity diffusionally than either thin cellular membranes or the skin. However, dimethylpolysiloxane membranes are essentially nonpolar and may be considered to closely approximate lipoid character. For this reason as well as the fact that dimethylpolysiloxane is itself used as an implant vehicle, dimethylpolysiloxane diffusional properties were extensively explored (1, 7, 9–12).

The studies of Garrett and Chemburkar (12) laid the groundwork for our own studies. These investigators showed the relative ease of passage of several classes of compounds through dimethylpolysiloxane films and, in particular, experimented extensively with *p*-aminopropiophenone, a closely related homolog of the permeant employed in the present studies. Because of a relatively insensitive method of following the diffusional process, they were not able to estimate lag times nor, consequently, apparent diffusivities and were, therefore, unable to distinguish between diffusivity changes and membrane solubility considerations when comparing the permeabilities of different species. These investigators wished to show that permeability constants could not be used predictively in lieu of diffusivities and indicated that lag times of about 7 hr. were to be expected for their system when the permeability coefficient was used in the calculation. This was then compared to their permeability plots which were linear and had intercepts not significantly different from zero (sampling times were in hours). Unfortunately, they solved for $t_L$ in seconds on the premise that the permeability constant could be in units of l./cm.-sec. when it must be in cm.²/sec., and this introduced a three order of magnitude error. Recalculation yields an expected lag time of 25.5 sec. This would not have permitted Garrett and Chemburkar (12) to make their desired point that substituting permeability constants for diffusion constants would give lag times inconsistent with their data. Lag times less than several minutes could not be observed with their technique. Their statement that a maximum undetectable displacement from zero intercept of 5 min. would force the apparent diffusivity to be greater than $10^{-8}$ l./cm.-sec. (*i.e.*, $10^{-5}$ cm.²/sec.) and the apparent partition coefficient to less than $10^{-2}$ should be changed to forcing the apparent diffusivity to be greater than $3.14 \times 10^{-11}$ l./cm.-sec. ($3.14 \times 10^{-8}$ cm.²/sec.) and the apparent partition coefficient less than 12. However, a lag time of 23 sec. would be predicted for the closely related diffusant, *p*-aminoacetophenone (1), and would be expected for *p*-aminopropiophenone under similar circumstances (37° and 76-μm. membrane). The coincidence of these values of 23 and 25.5 sec. results from the fortuitous fact that the apparent membrane/water partition coefficient of the propiophenone is close to 1.0[4]. The general conclusion of Garrett and Chemburkar (12) that Fick's first law is strictly obeyed in the dimethylpolysiloxane membrane systems is reinforced by the present experiments.

One major finding in these studies is that drug delivery from suspensions and solutions can be essentially controlled by the thermodynamic activity of the drug in the applied phase under carefully controlled conditions. This is an important feature of the "simplest case" diffusional model proposed by Higuchi (19) for topical adsorption. The standard state allowing the easiest interpretation of the phenomenon in this case is the crystalline solid. Any drug in solution which is in equilibrium with its solid necessarily (by definition) has a chemical potential equivalent to that of the solid. Therefore, all

[4] By extrapolation, $k_{app.}$ for the $C_2$ ketone is >0.15 in pure water. The π-value estimation ($\pi = 0.560$) yields a partition coefficient for the $C_3$ ketone of 0.545.

solutions up to $f_{PG}$ of 0.50 were of equivalent thermodynamic activity (directly related to chemical potential) with respect to the permeant and, since diffusivity adjusted fluxes were invariant within experimental error, the controlling influence on mass transport was the activity in the donor phase. This also is in accord with the studies of Garrett and Chemburkar (12) utilizing ethanol–water mixtures as a solvent system.

These data sharply contrast with those presented by Poulsen *et al.* (23) which were obtained using a seemingly similar system. Fluocinolone acetonide release from propylene glycol–water gels into isopropyl myristate was measured as a function of $f_{PG}$. These investigators found that maximum release for a fixed concentration of the steroid was obtained from "vehicles containing the minimum amount of propylene glycol necessary to dissolve the steroid completely." When a significant amount of undissolved drug was present, drug release rates plunged sharply, which was attributed to dissolution-rate control. Diffusion layers formed as the drug was leached from the gel were likely also contributive. These data have received wide acceptance, and it is generally believed that good topical drug availability depends on formulating to have full solution and also saturation. It is difficult to choose between thermodynamic control and dissolution-diffusion layer control as the best model for topical drug availability at this time. Poulsen (24) published some *in vivo* data consistent with the latter. Factors that point to this mechanism are the high viscosities of topical preparations and the lack of mixing at the surface of the skin (after initial application). However, the applied layer is extremely thin and many vehicles tend to dissolve in or fluidize on the skin surface. For a thin application of a fluid vehicle containing a drug with appreciable solubility, thermodynamic control is a distinct possibility. Further studies directed at unraveling this riddle are contemplated.

## REFERENCES


(1) G. L. Flynn and T. J. Roseman, *J. Pharm. Sci.*, **60**, 1788 (1971).

(2) J. T. Doluisio and J. V. Swintosky, *ibid.*, **53**, 597(1964).

(3) A. M. Agostini and J. H. Schulman, "Surface Activity and the Microbial Cell," 3rd ed., Gordon and Breach, New York, N. Y., 1965, p. 37.

(4) M. A. Augustine and J. Swarbrick, *J. Pharm. Sci.*, **59**, 314 (1970).

(5) J. Perrin, *ibid.*, **56**, 411(1967).

(6) M. H. Yunker and S. Borodkin, *ibid.*, **60**, 52(1971).

(7) G. L. Flynn and E. W. Smith, *ibid.*, **60**, 1713(1971).

(8) R. G. Stehle, doctoral thesis, University of Michigan, Ann Arbor, Mich., 1970.

(9) C. F. Most, *J. Appl. Polym. Sci.*, **11**, 1019(1970).

(10) T. J. Roseman and W. I. Higuchi, *J. Pharm. Sci.*, **59**, 353 (1970).

(11) J. Haleblian, R. Runkel, N. Mueller, J. Christopherson, and K. Ng, *ibid.*, **60**, 541(1971).

(12) E. R. Garrett and P. B. Chemburkar, *ibid.*, **57**, 944, 949 (1968).

(13) *Ibid.*, **57**, 1401(1968).

(14) K. Sundaram and F. A. Kincl, *Steroids*, **12**, 517(1968).

(15) H. A. Daynes, *Proc. Roy. Soc., Ser. A*, **97**, 286(1920).

(16) R. M. Barrer, *Trans. Faraday Soc.*, **35**, 628(1939).

(17) B. J. Zwolinski, H. Eyring, and C. E Reese, *J. Phys. Chem.*, **53**, 1426(1949).

(18) R. G. Stehle and W. I. Higuchi, *J. Pharm. Sci.*, **56**, 1367 (1967); see also *Reference 8*.

(19) T. Higuchi, *J. Soc. Cosmet. Chem.*, **11**, 85(1960).

(20) C. A. M. Hogben, D. J. Tocco, B. B. Brodie, and L. S. Schanker, *J. Pharmacol. Exp. Ther.*, **125**, 275(1959).

(21) A. Beckett and A. C. Moffatt, *J. Pharm. Pharmacol.*, **21**, 1445 (1969).

(22) R. J. Scheuplein, *J. Invest. Dermatol.*, **45**, 334(1965).

(23) B. J. Poulsen, E. Young, V. Coquilla, and M. Katz, *J. Pharm. Sci.*, **57**, 928(1968).

(24) B. J. Poulsen, *Brit. J. Dermatol., Suppl. 6*, **82**, 49(1970).


## ACKNOWLEDGMENTS AND ADDRESSES


Received April 26, 1971, from *The Upjohn Co., Kalamazoo, MI 49001*

Accepted for publication September 3, 1971.



▲ To whom inquiries should be directed.


# Toxicological and Pharmacological Studies on Sea Anemone, *Calliactis polypus* (Hormathiidae)


**C. L. HUANG*▲ and G. N. MIR†**



**Abstract** □ Tentacles of *Calliactis polypus* were homogenized and centrifuged, and the supernatant liquid was lyophilized. Mice receiving a phosphate buffer solution of the lyophilized material, ranging between 7.5 and 15.0 mg./kg. i.p., demonstrated a stuporous condition and respiratory distress; some died within 24 hr. The $LD_{50}$ in mice was 32 mg./kg. Doses of 5–15 mg./kg. produced a decrease in the blood pressure and bradycardia. These effects were abolished by bilateral vagotomy and atropinization. With higher doses, various arrhythmias and ECG abnormalities were observed. When tested on isolated rabbit heart, the extract caused a decrease in heart rate, force of contraction, and rate of coronary outflow. The extract produced contraction in the isolated rabbit duodenum, guinea pig ileum, and rat uterus by parasympathetic stimulation. These effects were abolished by atropine.



**Keyphrases** □ *Calliactis polypus* (sea anemone)—toxicology, pharmacology □ Sea anemone—toxicology, pharmacology □ Toxicity—*C. polypus* (sea anemone)


The sea anemone is one of the most abundant of the seashore animals. Approximately 1000 species are found in the ocean. They vary in size from a few millimeters to 0.5 m. or more in diameter. Most species are sessile and are attached to objects of various kinds but are, nevertheless, able to creep about to some extent. When they are covered by water and undisturbed, the body and tentacles have a flowerlike appearance (1).